3664–3673 *Nucleic Acids Research, 2001, Vol. 29, No. 17*

Determination of optimal sites of antisense oligonucleotide cleavage within *TNF*α mRNA

B. H. Lloyd*, R. V. Giles[1], D. G. Spiller[2], J. Grzybowski[2], D. M. Tidd[2] and D. R. Sibson

Clatterbridge Cancer Research Trust, J. K. Douglas Research Laboratories, Clatterbridge Hospital, Bebington, Wirral CH63 4JY, UK, [1]Department of Haematology and [2]School of Biological Sciences, University of Liverpool, Liverpool L69 7BZ, UK

Received April 12, 2001; Revised and Accepted July 16, 2001

ABSTRACT

Antisense oligonucleotides provide a powerful tool in order to determine the consequences of the reduced expression of a selected target gene and may include target validation and therapeutic applications. Methods of predicting optimum antisense sites are not always effective. We have compared the efficacy of antisense oligonucleotides, which were selected *in vitro* using random combinatorial oligonucleotide libraries of differing length and complexity, upon putative target sites within *TNF*α mRNA. The relationship of specific target site accessibility and oligonucleotide efficacy with respect to these parameters proved to be complex. Modification of the length of the recognition sequence of the oligonucleotide library illustrated that independent target sites demonstrated a preference for antisense oligonucleotides of a defined and independent optimal length. The efficacy of antisense oligonucleotide sequences selected *in vitro* paralleled that observed in phorbol 12-myristate 13-acetate (PMA)-activated U937 cells. The application of methylphosphonate:phosphodiester chimaeric oligonucleotides to U937 cells reduced mRNA levels to up to 19.8% that of the untreated cell population. This approach provides a predictive means to profile any mRNA of known sequence with respect to the identification and optimisation of sites accessible to antisense oligonucleotide activity.

INTRODUCTION

Antisense oligonucleotides (ODNs) are designed to hybridise to a specific mRNA sequence in order to prevent translation (1). Antisense reagents can be readily synthesised, are sequence specific and have the potential to down-regulate the expression of any mRNA of known sequence. They are useful for determining protein function and interactions (2–4). The potential of antisense for therapy has been developed using animal models and selective clinical trials (5,6). Therapeutic agents have now been approved (7).

The selection of effective antisense ODN sequences can be problematic. The majority of active antisense ODNs have been chosen either empirically, by trial and error or by the consideration of the thermodynamic or structural properties of the target mRNA. Empirical analyses may require the screening of up to 30–50 antisense compounds in a cellular environment (8,9). The number of oligonucleotide sequences analysed to select potent antisense compounds can be reduced by computer modelling. RNA secondary and tertiary structural constraints may sequester or occlude sites that are available for hybridisation with oligonucleotides, resulting in their inaccessibility. The application of RNA folding algorithms in addition to enzymatic and chemical reagent mapping approaches have been used to predict secondary structure formations. However, such protocols cannot predict either the tertiary structural interactions or the topological or steric constraints that influence the accessibility of antisense ODNs to the target mRNA and therefore may be unreliable (10–13).

In vitro methodologies that do not depend upon predetermined knowledge of RNA structure have been applied to the problem of oligonucleotide recognition of folded RNA. The synthesis of combinatorial oligonucleotide libraries of defined sequence has been performed by alkaline fragmentation of end-labelled RNA (14), or by partial DNase digestion of the corresponding DNA (15). The application of oligonucleotide arrays (16–18) and matrix-assisted laser desorption/ionisation time-of-flight (MALDI-TOF) mass spectrometry (19,20) has also been used.

Combinatorial oligonucleotide approaches have analysed the competitive hybridisation of target mRNA to either random (21) or semi-random (12,22) oligonucleotide libraries *in vitro*. Such experimentation has resulted in the identification of DNA sequences exhibiting high affinity and selectivity for target mRNAs, providing effective antisense reagents *in vivo* (12). There is a direct and significant correlation between the efficacy of oligonucleotides selected by such *in vitro* methodologies and the inhibition of the expression of the target sequence (23).

Random combinatorial oligonucleotide libraries of 10 (24) or 11 nt (22) have been used to identify sites accessible to heteroduplex formation, from which the sequences of 20 nt antisense oligonucleotide compounds have been extrapolated. However, optimisation of antisense oligonucleotide efficacy is not only dependent upon the target site, but is also dependent upon oligonucleotide length. We have taken an experimental

*To whom correspondence should be addressed. Tel: +44 151 343 4304; Fax: +44 151 343 1820; Email: bryonyl@ccrt.co.uk

approach that will permit the *in vitro* identification of accessible sites upon any mRNA transcripts that are amenable to the optimal hybridisation of antisense oligonucleotides, with respect to oligonucleotide length and efficacy.

MATERIALS AND METHODS

Construction and *in vitro* synthesis of RNA transcripts

The *TNF*α cDNA fragment of the plasmid pE4 (American Type Culture Collection/NIH repository, Rockville, MD) was amplified by PCR with AmpliTaq (Applied Biosystems, Warrington, UK) with 2.0 mM $MgCl_2$ using the following primer sequences: TNFF1, 5′-CAUCAUCAUCAUCAUTTCT-GCTCTAAAAGCTGCTG-3′ and TNFR1, 5′-CUACUACUAC-UACCTAAGCAACCTTAATTTCTCG-3′. cDNA was purified (QIAquick PCR purification kit, Qiagen Ltd, Crawley, UK) prior to treatment with uracil DNA glycosylase and cloning into pAMP1 (Gibco Ltd, Paisley, UK), according to the manufacturer's protocol, creating the plasmid pTNF8.

pTNF8 was linearised by *Bam*HI restriction and transcribed using the RiboMAX™ large scale RNA production system, T7 (Promega Corp., Madison, WI). cRNA was extracted with phenol:chloroform:isoamylalcohol (25:24:1) pH 4.5 and residual nucleotides removed (G-50 Sephadex Quick Spin Column, Boehringer Mannheim). RNA transcripts were stored as aliquots at –80°C until required.

RNase H mapping experiments

The 20mer, 16mer, 12mer and 8mer random oligonucleotide libraries were denatured (95°C for 5 min and cooled on ice) prior to addition to each respective RNase H assay. *TNF*α cRNA (10–25 pmol) was incubated with 500 fmol–500 nmol ODN library and 0.05 U μl^{-1} RNase H (Amersham Pharmacia Biotech UK Ltd, Little Chalfont, UK) in 400 µl Tris-based buffer (20 mM KCl, 10 mM $MgCl_2$, 0.1 mM EDTA, 0.1 mM DTT, 20 mM Tris–HCl pH 7.5) at 37°C, in the presence of 0.5 U μl^{-1} Prime RNase inhibitor (Helena BioSciences, Sunderland, UK). Triplicate RNase H assays (400 µl) were prepared, from which 50 µl aliquots were withdrawn at appropriate time points and purified by phenol:chloroform:isoamylalcohol (pH 7.5) extraction. The oligonucleotide library was removed by sephacryl chromatography (MicroSpin S200 HR columns, Amersham Pharmacia Inc.). cRNA fragments were harvested by ethanol precipitation in the presence of 20 µg ml^{-1} glycogen. RNA was dissolved in 50 µl DEPC-treated water and stored in 10 µl aliquots at –80°C

Primer extension analysis

Primer sequences were selected approximately every 200 nt along the length of the *TNF*α transcript. cDNA synthesis was initiated from 0.5 pmol 6-carboxyfluorescein (6-FAM)-labelled primer added to each aliquot of fragmented cRNA by 0.25 U SuperScript II reverse transcriptase (Gibco Ltd) according to the manufacturer's protocol (45°C for 50 min). cDNA was ethanol precipitated, resuspended in formamide loading buffer and analysed on a 6% denaturing polyacrylamide gel in a 377 Prism DNA sequencer (Applied Biosystems). Specific primer extension products were sized and the extent of their fluorescent activity evaluated, this being directly proportional to the integrated area of the fluorescent peak. Data analysis was performed using GeneScan v.3.1 software (Applied Biosystems).

Analysis of hybrid formation

Triplicate samples of *TNF*α cRNA (2 pmol) were incubated with 1 pmol HEX™-labelled ODN each, in 20 µl hybridisation buffer (50 mM NaCl, 5 mM $MgCl_2$, 1 mM Tris–HCl pH 7.4) at 37°C for 20 h. A 4 µl aliquot of loading buffer was added [15% (w/v) Ficoll, 0.25% (w/v) bromophenol blue and 0.25% (w/v) xylene cyanol] to appropriate ODN standards and samples prior to the loading on a native 15% (w/v) acrylamide gel. Samples were resolved by electrophoresis at 3 W using a TBM running buffer (44 mM Tris–borate, 1 mM $MgCl_2$) at <8°C. ODN:cRNA hybrids were visualised directly by fluorescence imaging using a FluorImager™ SI (Molecular Dynamics, Sunnyvale, CA), fitted with a 570 DF 30 filter and analysed using the ImageQuaNT™ applications software.

Oligodeoxynucleotide synthesis

Fluorescently tagged chimaeric methylphosphonodiester:phosphodiester ODNs were synthesised as previously described (25). The 20mer ODNs were composed of 6MP:8PO:5MP internucleoside linkages. Oligonucleotides were synthesised from phosphoramidites and methylphosphonamidites (Cambio, Cambridge, UK) using the slow 1 µmol cycle (version 1.23) on an Applied Biosystems 381A DNA synthesiser. A linker group [5′-amino-modifier C_6-TFA (Glen Research)] was included as the last cycle on the synthesiser. Base deprotection was achieved as described by Hogrefe *et al.* (26,27) extended over 72 h. Fluorescent tagging was achieved using 5(6)-carboxyfluorescein *N*-hydroxysuccinimide ester (Molecular Probes Inc., Cambridge, UK) (25).

Cell culture

U937 cells were cultured in RPMI 1640 medium supplemented with L-glutamine (Gibco Ltd) and 10% heat-inactivated FBS (Sera Lab, JRH Biosciences, West Sussex, UK). Cells were maintained in the exponential phase of growth by subculturing three times a week.

Reversible cell permeabilisation with streptolysin O (SLO)

U937 cells were permeabilised as described (25; http://www.liv.ac.uk/~giles). Exponentially growing cells were treated with 20 ng/ml phorbol 12-myristate 13-acetate (PMA) for 4 h before permeabilisation, to induce *TNF*α expression. Cells were washed and permeabilised by SLO in the presence of 20 µM oligodeoxynucleotide using ~7 U SLO per 5×10^6 cells in 200 µl buffer. Samples of ~5×10^5 cells were taken 1 h after the initiation of permeabilisation, for flow cytometric analysis (28). Cell sampling was repeated 3 h post-permeabilisation for mRNA and protein analysis.

RNA purification and analysis

RNA was extracted from cell pellets using the RNeasy midi kit (Qiagen Ltd). Total RNA yields and purity were determined by spectrophotometery and the integrity of the RNA confirmed by formaldehyde gel electrophoresis (29). Aliquots were stored at –80°C until required.

The levels of expression of *TNF*α and irrelevant control hypoxanthine phosphoribosyltransferase (HPRT) mRNAs were quantitated and normalised using a quantitative multiplex

RT–PCR assay as described previously (B.H.Lloyd and D.R.Sibson, manuscript in preparation). Essentially, serial $\log_{10}$ dilutions of both Δ*TNF*α and Δ*HPRT* synthetic RNA competicons (ranging from $1 \times 10^{2.75}$ to $1 \times 10^{5.5}$ and from $1 \times 10^{5.25}$ to 1×10^{8} copies per reaction respectively) were supplemented with a constant quantity of target total RNA (10 ng). RT–PCR was conducted using an Access RT–PCR system (Promega Corp., Madison, MA). Reverse transcription was primed using 25 pmol d $(T)_{17}$ prior to amplification mediated by 10 pmol HEX™-*HPRT* and 6-FAM™-*TNF*α primer sets per reaction. The reactions were subjected to 25 cycles of 30 s at 94°C and 2 min at 68°C with a final extension of 7 min at 68°C. Amplified cDNA fragments were detected and analysed by denaturing polyacrylamide gel electrophoresis as above.

The competicon:amplicon ratio was calculated by division of the integrated peak areas of the smaller synthetic competicon by that of the native PCR amplicon. The log of the ratio versus log of the competitor copy number was plotted. The point at which the plot crossed the ordinate axis at zero was interpolated to yield the approximate number of the copies of competitor and thus the approximate copies of target mRNA per ng total RNA (30).

Protein analysis

PMA-stimulated U937 conditioned media was collected by centrifugal removal of cells and stored at 4°C until required. The TNFα protein content present in the cell supernatants was determined using a Practica TNFα ELISA kit (Genzyme Diagnostics, Cambridge, MA) (sensitivity >3pg ml^{-1}).

RNA folding prediction

The minimal free energy structures of *TNF*α mRNA were estimated using the MFOLD algorithm (31). Results were visualised using SQUIGGLES output (Genetics Computer Group, Madison, WI). The RNA folding algorithm of Mathews *et al.* (32), provided data suitable for analysis by the OligoWalk module of RNAStructure 3.5 (33) to calculate $\Delta G^{\circ}_{overall}$.

Data presentation

The *TNF*α mRNA and protein levels were corrected for the viable number of cells present in the sample under study [mRNA or protein level = (normalised level detected by QRT–PCR or ELISA)/(number of viable cells in flow cytometry sample)]. Results are expressed as a function of the mean level of SLO-only control values ± standard deviation.

RESULTS

Detection of sites accessible to heteroduplex formation

RNA mapping experiments were undertaken using a complex 8mer, 12mer, 16mer and 20mer random oligonucleotide libraries containing 4^8, 4^{12}, 4^{16} and 4^{20} sequences, corresponding to 65536, 1.6777×10^7, 4.2949×10^9 and 1.0995×10^{12} individual oligonucleotide sequences respectively. The libraries used in this protocol consisted of unsubstituted phosphodiester oligonucleotides, with no internal fixed sequence positions. All possible sequences were synthesised with an equimolar base representation at each sequence position.

Bimolecular complexes, consisting of oligonucleotide: *TNF*α mRNA hybrids, provided a substrate for the endonucleolytic activity of RNase H, resulting in the cleavage of the RNA constituent of the heteroduplex (34,35). Sites of RNA cleavage were detected by reverse transcriptase-mediated primer-extension of the 3′ fragments using 5′ 6-FAM-labelled primer sequences (Fig. 1). Electrophoretic separation and subsequent data analysis permitted the identification of the position of RNA cleavage to single nucleotide resolution. Identification of efficient and susceptible sites of cleavage was performed with respect to reaction time, rather than by the end-point analysis of reaction products

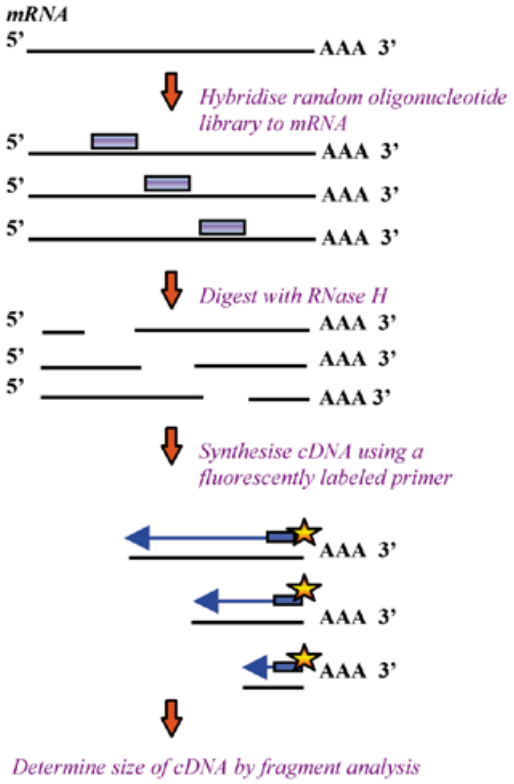

Figure 1. Approach used to detect sites accessible to potential antisense oligonucleotide hybridisation. An oligonucleotide library of a defined length is allowed to hybridise to *TNF*α mRNA. The RNA component of the DNA:RNA heteroduplex is cleaved by RNase H. The length of the fluorescent primer extension products, synthesised by reverse transcription, is defined by the sites of cleavage within the transcript. Cleavage site (nt) = position of 5′ terminus of the extension primer (nt) – length of cDNA (nt).

*TNF*α mRNA (16.5 pmol) was subject to RNase H cleavage analysis using 4 pmol 20mer ODN library, in a total volume of 400 µl. After a 20 min incubation period, the major proportion of the material consisted of full-length transcripts, suggesting that degradation was primarily mediated by single hybrid endonucleolysis. cDNA fragments were generated by the primer extension of RNA cleavage products resulting from 20mer ODN:RNA heterodimer-directed RNA cleavage at positions 99, 149 and 240 nt (Fig. 2A, fragments 1, 2 and 3 respectively). Reference profiles were provided by the primer extension products that were synthesised from full-length *TNF*α transcripts in the absence of RNase H (Fig. 2A and B, trace 1). Identical negative reaction profiles were also obtained in the absence of the oligonucleotide library (data not shown).

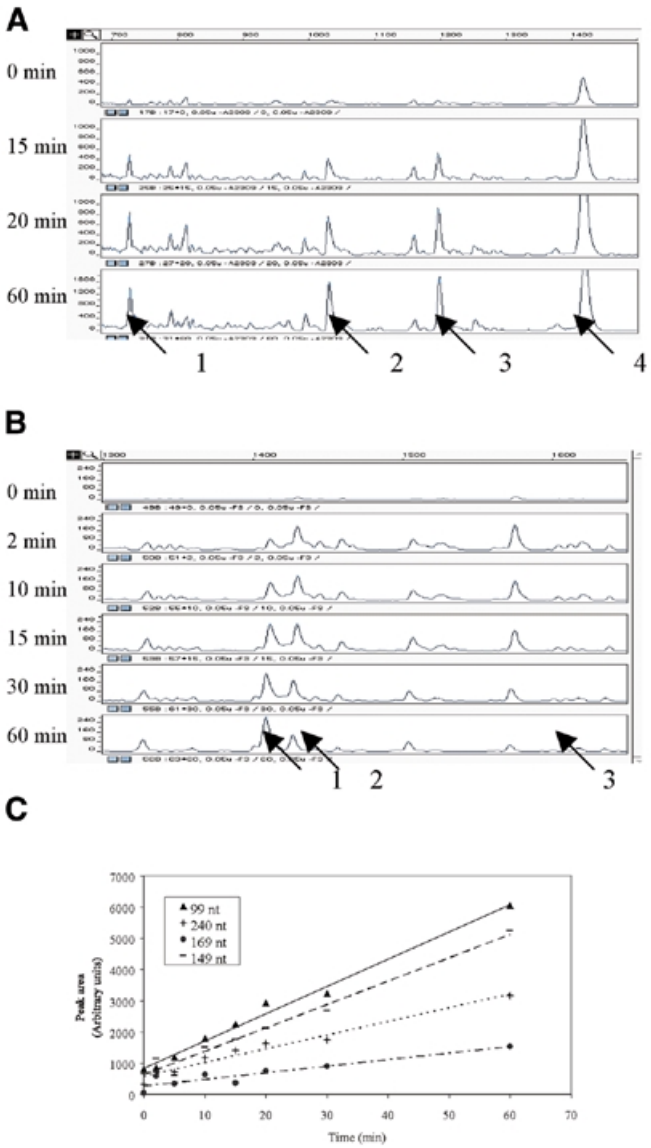

Figure 2. Electropherographic representations of RNA cleavage profiles detected by RNase H mapping and fluorescent primer extension. Cleavage of 16.5 pmol *TNF*α mRNA by 20mer oligonucleotide library (4 pmol) directed RNase H endolysis with respect to time. (**A**) Samples were analysed 0, 15, 20 and 60 min after the addition of RNase H. The fluorescent primer extension products represent fragments generated by cleavage at 240 (fragment 1), 149 (fragment 2) and 99 nt (fragment 3). Fragment 4 derives from the premature termination of reverse transcription at 40 nt. (**B**) The perturbation of primer extension by multiple transcript cleavage. Reaction conditions used are identical to those used in (A). Diminishing cDNA synthesis and apparent fragmentation result from a reduction in the ability to detect cleavage at upstream sites. Samples were analysed 0, 2, 10, 15, 30 and 60 min after the addition of RNase H. The fragments 1, 2 and 3 correspond to mRNA cleavage at 319, 314 and 275 nt respectively. (**C**) Analysis of coparallel RNA cleavage upon competitive hybridisation. The integrated peak areas of the primer extension fragments illustrated in (A) were plotted with respect to time.

The comparison of RNA cleavage data to the reference profiles (originating from experiments performed in the absence of either the oligonucleotide library or RNase H) ensured that the apparent fragmentation observed was derived from RNase H cleavage, as opposed to artifactual bands arising from the premature termination of the reverse transcription reaction (Fig. 2A, fragment 4).

The analysis of the yield of reaction products with respect to reaction time permitted the identification of false negative results. Such anomalies may arise from either excessive multiple transcript cleavage perturbing the primer extension reaction, or potential synergistic oligonucleotide annealing and subsequent cleavage of mRNA within the RNase H assay, this resulting from so called oligonucleotide 'facilitator functions' (36). An example of the deleterious effect of multiple transcript cleavage upon the visualisation of upstream sites is observed in Figure 2B. Cleavage of 16.5 pmol of the *TNF*α transcript in the presence of 4 pmol of the 20mer oligonucleotide library (using a reaction volume of 400 µl) illustrated that cleavage at 314 and 275 nt (Fig. 2B, fragments 2 and 3) occurs at a greater efficiency than that at the 319 nt site (Fig. 2B, fragment 1) after a 2 min incubation period (Fig. 2B, trace 2). However, after 60 min (Fig. 2B, trace 6) the cleavage of the transcript at 319 nt was sufficient to terminate the majority of primer extension reactions. This limited the ability of the reverse transcription reaction to access upstream sequences. The prevention of transcript read-through resulted in the under-representation of the efficiency of subsequent 3′ cleavage sites, as was illustrated by the apparent reduction in efficacy of RNA cleavage at 314 and 275 nt relative to the 319 nt site. This phenomenon would not have been apparent if the reaction had been subject to a single end-point analysis.

The relative efficiency of transcript cleavage was determined by plotting the integrated peak area of the fluorescent primer extension products with respect to reaction time (Fig. 2C). The efficiency of the extension reaction is dependent upon the affinity of the primer sequence for the target mRNA. Therefore, site-specific cleavage rates were analysed relative to those within a data set defined by the specific primer sequence used.

Assuming that RNA cleavage is mediated by one hit kinetics, the accessibility and susceptibility of the RNA to oligonucleotide hybridisation and subsequent RNase H endolysis at any given site dictates the rate of reaction. Therefore, the rate of reaction was directly proportional to the gradient of the resulting plot. The combinatorial oligonucleotide hybridisation assay identified numerous sites demonstrating a varying efficiency of hybrid formation and subsequent RNase H accessibility and processivity. For example, RNA cleavage at the sites illustrated in Figure 2A was ordered 99 > 149 > 240 > 169 nt, for which respective gradients representing the rate of synthesis of fluorescent primer-extended fragments of 87.36, 72.43, 41.28 and 18.41 arbitrary U min^{-1} were obtained respectively (Fig. 2C).

Effect of oligonucleotide length upon *in vitro* assays

Comparative RNA cleavage assays were performed using 20 pmol cRNA for each assay and 6 nmol random phosphodiester oligonucleotide libraries of either 8, 12, 16 or 20 nt in length in a reaction volume of 400 µl, from which 50 µl aliquots were withdrawn at appropriate time points. Each assay was performed in triplicate. After a 2 min incubation period, the samples were purified and subject to primer extension analysis. The resolution of the resulting cDNA fragments demonstrated that the efficiency of RNA cleavage was dependent upon the length of the oligonucleotide library

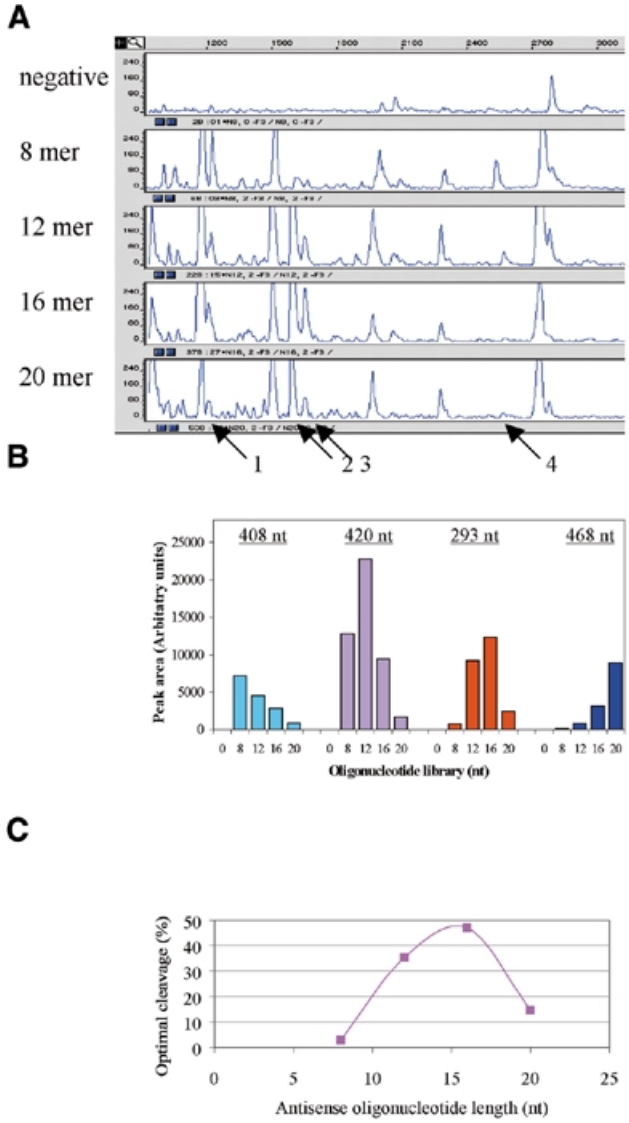

Figure 3. Efficacy of RNA cleavage with respect to random oligonucleotide library length. (**A**) Electropherographic traces from fluorescent primer-extended RNA fragments (generated from 20 pmol *TNF*α mRNA) were derived from RNase H assays using 6 nmol of either the 8mer, 12mer, 16mer or 20mer oligonucleotide libraries, as compared to an RNase H negative control. Sites demonstrating preferential cleavage with respect to oligonucleotide length were identified at 408 (fragment 1), 308 (fragment 2), 293 (fragment 3) and 51 nt (fragment 4). (**B**) Integrated peak area of individual primer-extended RNA fragments plotted with respect to oligonucleotide length. Preferential site-specific cleavage at 408 (light blue bars), 420 (purple bars), 293 (red bars) and 468 nt (dark blue bars) was observed using the 8mer, 12mer, 16mer and the 20mer ODN libraries respectively. (**C**) The number of sites demonstrating maximal specific cleavage for each oligonucleotide library was analysed, expressed as a percentage of the total and plotted with respect to oligonucleotide length.

employed in the RNase H assay (Fig. 3A). Cleavage of *TNF*α RNA at 308 and 293 nt (Fig. 3A, fragments 2 and 3 respectively) demonstrated an optimal reaction efficiency when a random oligonucleotide library of 16mers was employed. Conversely, when using an oligonucleotide library of 8mers, maximal RNA cleavage at 408 and 51 nt (Fig. 3A, fragments 1 and 4 respectively) was observed. The dependence of the cleavage reaction efficiency with respect to oligonucleotide length was such that the latter fragment, resulting from cleavage at 51 nt, was only observed when oligonucleotide libraries of 8mers and 12mers were analysed. Cleavage of the RNA at position 51 nt could not be detected when using oligonucleotide libraries of 16 or 20 nt in length.

The integrated peak area of the resultant cDNA fragments for each cleavage product was plotted with respect to the length of the oligonucleotide library used for each assay. For every detectable site, the efficiency of site-specific cleavage was dependent upon the length of the combinatorial oligonucleotide library employed. For example, preferential site-specific cleavage was observed using the 8, 12, 16 and 20 nt random oligonucleotide libraries at 408, 420, 293 and 468 nt respectively (Fig. 3B).

Thirty-four sites upon the 1585 nt transcript were accessible to ODN hybridisation and subsequent RNase H-mediated cleavage. Comparison of the site-specific cleavage data with respect to oligonucleotide length illustrated that maximal cleavage for the 8mer, 12mer, 16mer and 20mer libraries was favoured at 2/34 (5.9%), 12/34 (35.3%), 16/34 (47%) and 5/34 (14.7%) of the sites analysed respectively (Fig. 3C). Therefore, the efficacy of *in vitro* site-specific cleavage was ordered with respect to the complexity of random combinatorial oligonucleotide libraries as follows: 16mers > 12mers > 20mers > 8mers.

Selection of antisense sites

Two sites illustrating differing hybrid degradation efficiencies were selected for *in vivo* analysis: one site at 99 nt demonstrated a high degree of susceptibility to cleavage, the second site at 877 nt being relatively refractory to cleavage [antisense (As)4 and As1 respectively]. In addition, two antisense oligonucleotides were targeted to sites demonstrating an intermediate cleavage response *in vitro* were also analysed: these were located at positions 1307 and 1538 nt upon the cRNA transcript (As2 and As3 respectively). The relative efficiencies of transcript cleavage were calculated by determining the gradients obtained by plotting the integrated peak area of the fluorescent primer extension reaction products with respect to reaction time (Fig. 4A). Determination of the relative efficiencies of transcript cleavage for As1–As4 resulted in values of 3.79, 51.37, 32.31 and 87.36 arbitrary U min^{-1} respectively.

The position of the antisense oligonucleotides with respect to the calculated minimal free-energy structures of *TNF*α mRNA is illustrated in Figure 4B. Two of the oligonucleotides selected by competitive hybridisation assays (As1 and As4) were predicted to target loops of hairpin regions, whilst As2 and As3 were predicted to hybridise to duplex regions, the former duplex being interrupted by internal looped regions. The sequence of 20mer oligonucleotides used in this study and chemical modifications thereof are presented in Table 1.

Oligonucleotide affinity

The relative affinity of unsubstituted oligonucleotides for their target RNA sequence was determined by hybrid analysis using a gel shift assay. The affinity of phosphodiester ODN sequences, corresponding to As1–As4, to the *TNF*α transcript was determined, as was that for their inverse polarity sequence counterparts [inverse antisense (iAs)1–iAs4]. Unlabelled RNA

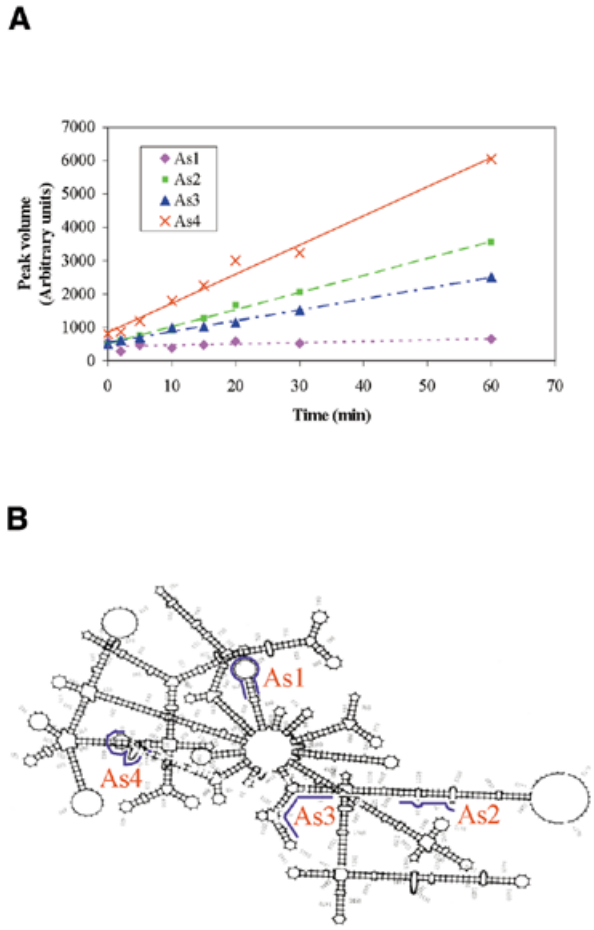

Figure 4. Predicted efficacy and location of As1–As4. (**A**) The integrated peak areas of the fluorescent primer-extension products, generated at sites corresponding to those targeted by As1–As4, was plotted with respect to time. *TNF*α mRNA (16.5 pmol) was hybridised to 4 pmol random 20mer ODN library in the presence of RNase H. Resulting fragments were visualised by FAM-labelled primer extension and subsequent fragment analysis. (**B**) Location of antisense oligonucleotides As1–As4, with reference to a predicted secondary structure plot of *TNF*α mRNA. The minimal free energy structure of *TNF*α mRNA was estimated using the MFOLD algorithm (31).

(2 pmol) was incubated in the presence of HEX-labelled oligonucleotides (1 pmol) at 37°C for 20 h. The resulting hybrids were resolved by non-denaturing polyacrylamide gel electrophoresis prior to detection and quantitation by fluorimagery.

The affinity of the oligonucleotides for the target sequence, as determined by the quantity of ODN:RNA heterodimeric species formed *in vitro* (Table 2), corresponded to the rate of transcript cleavage observed in the RNase H assay, i.e. As4 > As2 > As3 > As1. Hybrid formation between the *TNF*α mRNA transcript and the inverse polarity antisense ODN sequences (iAs1–iAs4) was not detected. Therefore, the rate of RNase H-mediated cleavage observed in the *in vitro* assay is primarily dependent upon both the accessibility and affinity of sites within the transcript to form RNA:ODN hybrids, rather than as a function of the site specific accessibility and processivity of RNase H alone.

Efficacy of selected antisense oligonucleotides *in vivo*

To direct the activity of RNase H *in vivo*, methylphosphonate:phosphodiester chimaeric antisense oligonucleotides were synthesised to incorporate the sites demonstrating cleavage *in vitro* within the internal phosphodiester element of the chimaera (Table 1). Methylphosphonate oligodeoxynucleotide derivatives are refractory to RNase H endonucleolysis. As little as a 6 base complementarity region of an unsubstituted phosphodiester oligomer to target is sufficient to elicit human RNase H1 activity (37), therefore a central 8 base phosphodiester element was included in the design of the antisense compounds.

The expression of *TNF*α mRNA by the human monocytic leukaemia cell line U937 was stimulated by incubating the cells in the presence of 20 ng ml^{-1} PMA for 4 h. As and iAs methylphosphonate:phosphodiester oligodeoxynucleotides were introduced into the cell cytoplasm by SLO-mediated reversible permeabilisation of the cell membrane in the presence of a 20 μM extracellular concentration of oligomer. After oligonucleotide addition and a subsequent 3 h incubation, the expression levels of *TNF*α mRNA and protein were determined by QC RT–PCR and ELISA respectively (Fig. 5). The permeabilisation of U937 cells with SLO did not significantly perturb the level of PMA-induced *TNF*α mRNA or protein synthesis when compared to PMA-stimulated cells alone (1.15×10^4 *TNF*α transcripts ng^{-1} total RNA ± 1450 and 1.19×10^4 ± 1560 transcripts ng^{-1} total RNA; 69.1 pg ml^{-1} ± 6.36 and 67.8 pg ml^{-1} ± 4.2 TNFα protein respectively).

Incubation of permeabilised U937 cells in the presence of As1–As4 resulted in the respective reduction of *TNF*α mRNA to 107.3 ± 8.2, 52.7 ± 13.2, 59.7 ± 14.4 and 19.8 ± 4.7% that of the SLO-treated induced control (Fig. 5A). The respective oligonucleotide efficacy, with respect to mRNA expression levels, can be ordered as follows: As4 > As2 > As3 > As1. Similarly, upon the antisense oligonucleotide treatment of U937 cells, the decrease of TNFα protein synthesis (Fig. 5B) was as follows: As4 > As2 > As3 > As1 (44.9 ± 8.6, 104.4 ± 13.33, 136.48 ± 14.4 and 206.8 ± 8.22% respectively).

Upon the application of the reverse polarity control sequences iAs1–iAs4, a respective induction of TNFα protein synthesis was observed, 188 ± 20, 148.8 ± 16.6, 199.4 ± 6.6 and 186 ± 4.6% that of SLO-permeabilised PMA-stimulated cells alone.

Specificity of antisense oligomers

To ensure that the suppression of *TNF*α mRNA and protein was the result of sequence specific antisense effects, the samples were examined for non-target mRNA expression. The treatment of U937 cells with the *TNF*α antisense and inverse antisense reagents did not result in any consequential perturbation of non-target HPRT mRNA levels after SLO-mediated delivery of methylphosphonate:phosphodiester chimaeric oligodeoxynucleotides, relative to control SLO-treated, PMA-induced samples (Fig. 5C). HPRT levels of antisense oligodeoxynucleotide-treated cells were between 106.2 ± 8.87 and 92.4 ± 15.3% that expressed by the induced, SLO-permeabilised cells.

Table 1. Structure of methylphosphonate:phosphodiester chimaeric oligonucleotides

Oligonucleotide	Position[b]	Sequence and structure (5′→3′)[a,b]
Antisense		
As1	886–867	F~$T_mG_mG_mA_mG_mA_oA_oG_oA_oC_oC_oG_oA_oG_mT_mT_mT_mT_mC$
As2	1316–1297	F~$A_mT_mA_mA_mA_mC_oC_oC_oT_oC_oT_oG_oG_oC_mC_mC_mC_mA_mT_mA$
As3	1547–1528	F~$A_mC_mA_mC_mA_mG_oA_oC_oA_oT_oT_oA_oG_oC_mC_mG_mG_mA_mT_mG$
As4	99–80	F~$C_mT_mG_mT_mG_mG_oT_oA_oC_oT_oC_oG_oT_oG_mA_mC_mT_mT_mT_mC$
Inverse antisense		
iAs1	n.a.	F~$C_mT_mT_mT_mT_mT_mG_oA_oG_oC_oC_oA_oG_oA_oA_mG_mA_mG_mG_mT$
iAs2	n.a.	F~$A_mT_mA_mC_mC_mC_mC_oG_oG_oT_oC_oT_oC_oC_oC_mA_mA_mA_mT_mA$
iAs3	n.a.	F~$G_mT_mA_mG_mG_mC_mC_oG_oA_oT_oT_oA_oC_oA_oG_mA_mC_mA_mC_mA$
iAs4	n.a.	F~$C_mT_mT_mT_mC_mA_mG_oT_oG_oC_oT_oC_oA_oT_oG_mG_mT_mG_mT_mC$

n.a., not applicable.
[a]ODN sequences used to repress the *TNF*α expression of PMA-stimulated U937 cells.
[b]Antisense oligonucleotide sequences are complimentary to 'HSTNFAA', GenBank accession no. M10988.
[c]Internucleoside linkages and termini: o, phosphodiester; m, methylphosphonate; F~, 5(6)carboxyfluorescein-aminohexanol

Table 2. Relative affinity of ODN for *TNF*α mRNA

Oligonucleotide ID[a]	ODN:cRNA heteroduplex (fmol)[b]
As1	n.d.[c]
As2	5.27 ± 0.75
As3	2.91 ± 0.45
As4	9.40 ± 0.66
iAs1	n.d.
iAs2	n.d.
iAs3	n.d.
iAs4	n.d.

[a]HEX-labelled, unsubstituted phosphodiester ODN.
[b]Quantity of ODN forming ODN:cRNA heteroduplexes upon the incubation of 2 pmol cRNA with 1 pmol HEX™-labelled ODN at 37°C for 20 h ± standard deviation.
[c]n.d., not detected.

Comparison of oligonucleotide efficacy with predictive parameters

The levels of the predicted antisense oligonucleotide activities of the methylphosphonate:phosphodiester chimaeric ODNs As1–As4 (as determined using the phosphodiester 20mer ODN library in an *in vitro* RNase H assay) were compared to the actual activities observed upon the levels of *TNF*α mRNA and protein expressed by activated U937 cells when treated with the antisense ODNs. A direct inverse correlation was found between the predicted antisense activity and the resultant levels of *TNF*α mRNA and protein expression (respective correlation coefficients of –0.98 and –0.99) (Fig. 6A).

A comparison of the efficacy of As1–As4 with predictive calculated thermodynamic parameters found no significant correlation between ODN efficacy and either ΔG calculations of the oligo-target binding from unstructured states (illustrative of duplex stability) or T_m estimations (correlation coefficients of 0.55 and 0.91 respectively). However, a direct linear proportionality was observed between the activity of As1–As4 *in vivo* and $\Delta G^\circ_{overall}$ (correlation coefficient = 0.99) (Fig. 6B). $\Delta G^\circ_{overall}$ was calculated using OligoWalk option within RNA Structure v.3.5 programme (33) and is defined as the net ΔG (kcal/mol) of oligo-target binding, when all contributions are considered, including breaking target structures and oligonucleotide intramolecular secondary structural formations, if any. OligoWalk predictions of oligonucleotide-target affinity resulted in $\Delta G^\circ_{overall}$ values ranging from –18.9 to +2.6 kcal/mol.

DISCUSSION

Highly specific and reproducible cleavage of the target mRNA was observed using *in vitro* RNase H assays utilising either of the 8mer, 12mer, 16mer or the 20mer random oligonucleotide libraries. Selective ODN:RNA competitive hybridisation was evident within the highly redundant sequences of each of the libraries tested, resulting in characteristic and comparable inter-library RNA fragmentation profiles. From the data obtained, both the predicted sequence and relative potency of potential antisense oligonucleotides were derived.

Analysis of the resultant *in vitro* data identified 34 sites upon the *TNF*α mRNA that are accessible to oligonucleotide hybridisation and subsequent cleavage within the 1585 nt transcript; corresponding to an approximate frequency of one site per 47 RNA residues.

The screening of multiple oligonucleotide sequences (often 30–50 and up to 100) in cells is usually required for the discovery of a few active antisense sequences. Such intensive oligonucleotide walking experiments have been effective for a number of mRNAs of therapeutic interest (38–40). By comparison, the co-parallel selection of oligonucleotides *in vitro* provides an efficient methodology for predicting the efficacy of potential antisense reagents and limiting the number candidate sequences to be assessed *in vivo*.

Optimisation of antisense oligonucleotide efficacy *in vitro* is dependent upon both the selection of the mRNA target site and

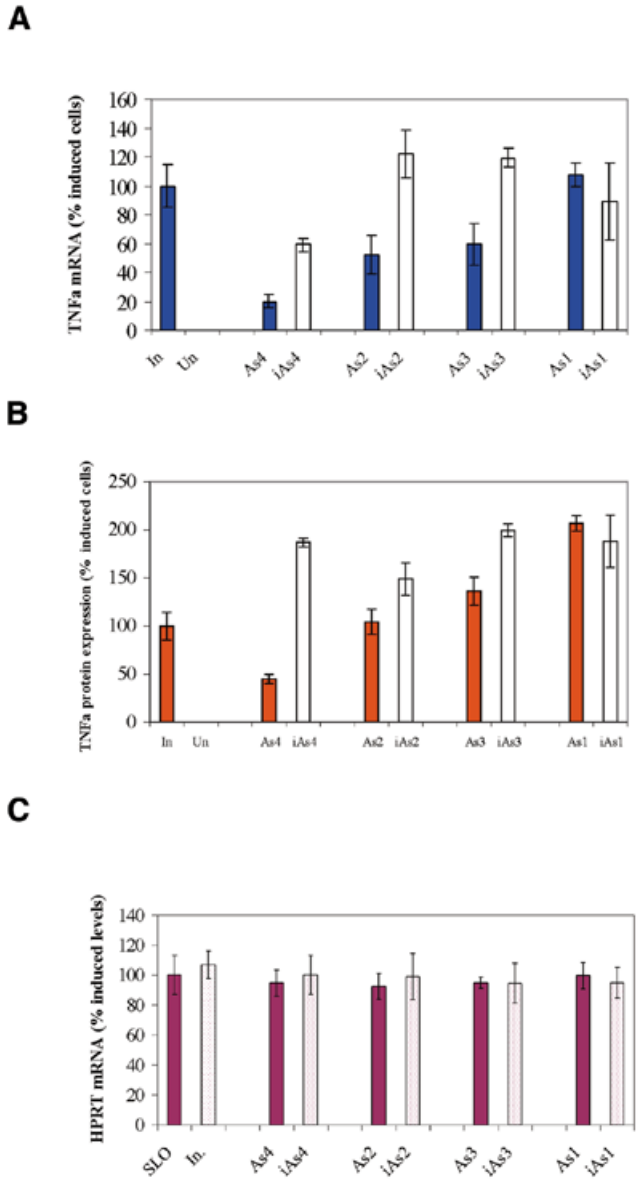

Figure 5. Efficacy of antisense oligonucleotide activity. Data is expressed as a function of the levels expressed by the PMA-induced SLO-permeabilised cell control. In, PMA-induced U937 cells; Un, non-induced non-permeabilised U937 cells; SLO, PMA-induced SLO-permeabilised U937 cells. (**A**) *TNF*α mRNA expression was determined by absolute quantitative competitive RT–PCR. (**B**) TNFα protein levels determined by ELISA. (**C**) HPRT mRNA expression was analysed by absolute quantitative competitive RT–PCR.

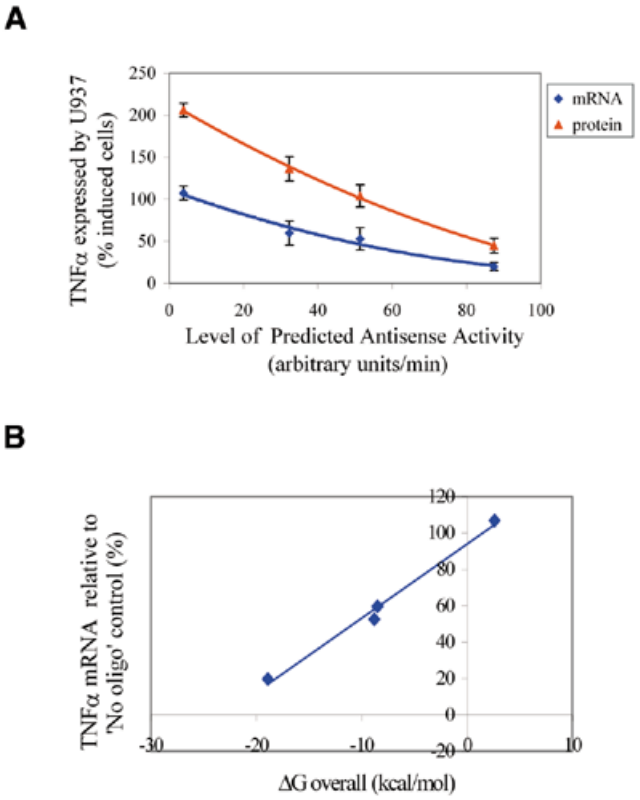

Figure 6. Correlation of antisense oligonucleotide efficacy with predictive methods. (**A**) Correlation of antisense oligonucleotide efficacy *in vivo* with activity observed *in vitro*. The level of predicted antisense activity corresponded to the rate of cleavage of RNA:DNA hybrids observed when using the 20mer ODN libraries at sites corresponding to sequences targeted by As1–As4, as determined using *in vitro* RNase H assays. The rate of cleavage was plotted with respect to the levels of *TNF*α mRNA and protein expressed by PMA-activated U937 cells upon the application of methylphosphonate:phosphodiester chimaeric ODN derivatives (as determined by QC RT–PCR and ELISA respectively). (**B**) Antisense oligonucleotide efficacy with respect to $\Delta G^{\circ}_{overall}$. $\Delta G^{\circ}_{overall}$ of As1–As4 was calculated using the OligoWalk module of RNAstructure 3.5 (33).

the length of the individual antisense compound used. It is difficult to predict the degree to which antisense oligomers will cause site-specific degradation of RNA. RNA:ODN hybridisation relies upon the kinetic and thermodynamic parameters of RNA folding, oligonucleotide affinity and association and dissociation rates. The short recognition sequence of the random 8mer oligonucleotides used is expected to result in relatively weak ODN binding to the transcript and fast dissociation, forming less stable RNA:ODN complexes. RNA:ODN complex instability will discriminate against RNase H activity (40). As the recognition sequence was lengthened, the dissociation of both matched and mismatched hybrids is expected to decrease, resulting in a concurrent increase in RNase H endonucleolysis. However, extrapolation of the theoretical premise of linear hybridisation thermodynamics needs to consider the potential energetic costs incurred in breaking intramolecular bonds prior to the formation of ODN:RNA heterodimers. The greater the length of the recognition sequence, the greater the probability that the target site has been sequestered by secondary or tertiary structural interactions, limiting oligonucleotide accessibility. This is consistent with our experience where increasing the recognition sequence of the random oligonucleotide library from 16mer to 20mer resulted in maximal RNA cleavage at only 14.7% of the target sites identified, as opposed to 47% for the 16mer library. The specific inhibition of gene expression has been observed using oligonucleotides as small as 7 and 8 nt (41). However, the potency of the heptanucleotide compound was some 6-fold less than that of a previously described 20 nt antisense inhibitor (42).

The identification of sites demonstrating complex cleavage can be determined by the temporal monitoring of the development of the RNA fragmentation profile. For example, the secondary and tertiary structure of the transcript may be

disrupted by oligonucleotide stand displacement or effectively null sites may become susceptible to secondary cleavage once unmasked by a primary cleavage event. Further complications may arise with the potential for the multiple turnover of oligonucleotides in combinatorial assays. This has been implicated at sites of high affinity and hybridisation rate where the library concentration is theoretically limiting (21). The identification of target sites that are susceptible to such anomalous cleavage should help to prevent the design and application of independent antisense compounds that demonstrate relatively little activity *in vivo*. Target sites demonstrating such a false positive reaction can be selected against when monitoring the evolution of the RNA fragmentation profile.

Data resulting from the *TNF*α mRNA RNase H competitive hybridisation assays permitted the selection and synthesis of four 20mer methylphosphonate:phosphodiester chimaeric antisense oligonucleotides (As1–As4) shown to exhibit differing activity *in vitro* (As4 > As2 > As3 > As1). The efficacy of the antisense oligonucleotides was compared to that of their respective reverse polarity counterparts, iAs1–iAs4. Hybrid analysis of As1–As4:*TNF*α mRNA heterodimer formation has shown there to be a direct correlation between the relative oligonucleotide affinity at equilibrium and the corresponding rate of transcript cleavage *in vitro*. When tested in the PMA-activated monocytic cell line U937, the efficacy of the antisense oligonucleotides *in vivo* directly correlated to that observed *in vitro*. The reduction in both the levels of mRNA and protein synthesised by U937 cells was ordered as follows: As4 > As2 > As3 > As1. As4 reduced the respective levels of *TNF*α mRNA and protein to that of 19.8 ± 4.7 and 44.9 ± 8.6% that of the untreated, PMA-stimulated control, whilst As1 was effectively inactive. For all of the antisense sequences analysed, the inhibition of *TNF*α mRNA expression was greater than that observed for TNFα protein synthesis. The greater reduction of *TNF*α mRNA compared to protein levels is not unexpected, as *TNF*α mRNA has a shorter half-life and therefore a more rapid turnover (43). Neither the reversible permeabilisation of U937 cells with SLO nor the addition of the antisense compounds to the cells had a significant effect upon the level of HPRT mRNA expression. The results are illustrative of the low toxicity of SLO permeabilisation of U937 cells and the specificity of the *TNF*α antisense reagents.

Interestingly, a marked stimulation of TNFα protein synthesis was observed upon the addition of inverse antisense methylphosphonate:phosphodiester chimaeric oligonucleotides to PMA-stimulated U937 cells. A reduction in the expression of TNFα protein levels, relative to the PMA-activated, untreated control cells, could only be detected using the most potent antisense oligonucleotide, As4. The level of oligonucleotide mediated TNFα augmentation was independent of specific, embedded sequence motifs that may result in either the stimulation of immune cells or correlate to poor antisense oligonucleotide efficacy (44,45). The stimulation of TNFα protein synthesis may be the result of a reaction to the oligonucleotide chemistry. The addition of phosphorothioate oligonucleotides to lipopolysaccharide-stimulated cells has been seen to result in the non-sequence specific augmentation of TNFα synthesis (46–48). Methylphosphonate:phosphodiester chimaeric antisense compounds, when added to PMA-induced cells, appeared to produce a similar response.

A comparison of the competitive hybridisation *in vitro* assay with alternative methods of predicting oligonucleotide efficacy found the following: (i) The delineation of oligonucleotides upon minimal free energy structure predictions of *TNF*α mRNA provided results that were difficult to interpret. The results inferred that both highly effective and inactive oligonucleotides (As4 and As1 respectively) target assumedly accessible open loop structures. (ii) Calculated ΔG° values or T_m predictions provided only a moderate correlation with respect to the inhibition of TNFα synthesis *in vivo*, whilst $\Delta G^\circ_{overall}$ predictions appeared to be the most accurate in this assay. (iii) Prospective antisense experiments with rat *TNF*α mRNA (49) have shown that oligonucleotides that contain the TCCC motif had a much higher success rate (50%) than those selected by trial and error (6%). The embedded sequence motif TCCC was present within As2, the addition of which resulted in a moderate decrease in *TNF*α mRNA levels (52.7% that of untreated cells). Although As2 has been shown to result in TNFα inhibition, As4, the most potent of all of the oligonucleotides tested, was free of any significant sequence moiety known to date (50).

Data originating from *in vitro* RNase H assays employing semi-random oligonucleotide libraries of limited complexity (11 nt) has been extrapolated to define sites suitable for the design of antisense compounds of 20 nt in length (22). However, such a universal extrapolation may not always be applicable and may be subject to misrepresentation when using an oligonucleotide library of a smaller size and complexity.

The ability of the *in vitro* assay to predict oligonucleotide efficacy was superior to either computationally based RNA structural predictions, ΔG calculations and *in vivo* trial and error methodologies. Such results are illustrative of the potential of the coparallel competitive screening of the *in vitro* selection methodology to predict effective antisense oligonucleotide sequences.

ACKNOWLEDGEMENTS

We thank Dr N. Halliwell for invaluable technical assistance. This work was supported by the Clatterbridge Cancer research Trust and the Leukaemia Research Fund.

REFERENCES

1. Helene,C. and Toulme,J.J. (1990) Specific regulation of gene expression by antisense, sense and antigene nucleic acids. *Biochim. Biophys. Acta*, **1049**, 99–125.
2. Deszo,E.L., Brake,D.K., Cengel,K.A., Kelley,K.W. and Freund,G.G. (2001) CD45 negatively regulates monocytic cell differentiation by inhibiting PMA-dependent activation and tyrosine phosphorylation of PKCδ. *J. Biol. Chem.*, **276**, 10212–10217.
3. Chu,Z.L., Pio,F., Xie,Z., Welsh,K., Krajewska,M., Krajewski,S., GodzikA. and Reed,J.C. (2001) A novel enhancer of the Apaf1 apoptosome involved in cytochrome c-dependent caspase activation and apoptosis. *J. Biol. Chem.*, **276**, 9239–9245.
4. Al-Alwan,M.M., Rowden,G., Lee,T.D. and West,K.A. (2001) Fascin is involved in the antigen presentation activity of mature dendritic cells. *J. Immunol.*, **166**, 338–345.
5. Kushner,D.M. and Silverman,R.H. (2000) Antisense cancer therapy: the state of the science. *Curr. Oncol. Rep.*, **21**, 23–30.
6. Cotter,F.E., Waters,J. and Cunningham,D. (1999) Human Bcl-2 antisense therapy for lymphomas. *Biochim. Biophys. Acta*, **1489**, 97–106.
7. de Smet,M.D., Meenken,C.J. and van den Horn,G.J. (1999) Fomivirsen–a phosphorothioate oligonucleotide for the treatment of CMV retinitis. *Ocul. Immunol. Inflamm.*, **7**, 189–198.

8. Monia,B.P., Johnston,J.F., Geiger,T., Muller,M. and Fabbro,D. (1996) Antitumor activity of a phosphorothioate antisense oligodeoxynucleotide targeted against C-raf kinase. *Nature Med.*, **2**, 668–675.
9. Dean,N.M., McKay,R., Condon,T.P. and Bennett,C.F. (1994) Inhibition of protein kinase C-α expression in human A549 cells by antisense oligonucleotides inhibits induction of intercellular adhesion molecule 1(ICAM-1) mRNA by phorbol esters. *J. Biol. Chem.*, **269**, 16416–16424.
10. Sczakiel,G., Homann,M. and Rittner,K. (1993) Computer-aided search for effective antisense RNA target sequences of the human immunodeficiency virus type 1. *Antisense Res. Dev.*, **3**, 45–52.
11. Laptev,A.V., Lu,Z., Colige,A. and Prockop,D.J. (1994) Specific inhibition of expression of a human collagen gene (COL1A1) with modified antisense oligonucleotides. The most effective target sites are clustered in double-stranded regions of the predicted secondary structure for the mRNA. *Biochemistry*, **33**, 11033–11039.
12. Ho,S.P., Bao,Y., Lesher,T., Malhotra,R., Ma,L.Y., Fluharty,S.J. and Sakai,R.R. (1998) Mapping of RNA accessible sites for antisense experiments with oligonucleotide libraries. *Nat. Biotechnol.*, **16**, 59–63.
13. Patzel,V., Steidl,U., Kronenwett,R., Haas,R. and Sczakiel,G. (1999) Theoretical approach to select effective antisense oligodeoxyribonucleotides at high statistical probability. *Nucleic Acids Res.*, **27**, 4328–4334.
14. Rittner,K., Burmester,C. and Sczakiel,G. (1993) *In vitro* selection of fast-hybridizing and effective antisense RNAs directed against the human immunodeficiency virus type 1. *Nucleic Acids Res.*, **21**, 1381–1387.
15. Matveeva,O., Felden,B., Audlin,S., Gesteland,R.F. and Atkins,J.F. (1997) A rapid *in vitro* method for obtaining RNA accessibility patterns for complementary DNA probes: correlation with an intracellular pattern and known RNA structures. *Nucleic Acids Res.*, **25**, 5010–5016.
16. Milner,N., Mir,K.U. and Southern,E.M. (1997) Selecting effective antisense reagents on combinatorial oligonucleotide arrays. *Nat. Biotechnol.*, **15**, 537–541.
17. Ramsay,G. (1998) DNA chips: state-of-the-art. *Nat. Biotechnol.*, **16**, 40–44.
18. Sohail,M. and Southern,E.M. (2000) Antisense arrays. *Mol. Cell Biol. Res. Commun.*, **3**, 67–72.
19. Bleczinski,C.F. and Richert,C. (1998) Monitoring the hybridization of the components of oligonucleotide mixtures to immobilized DNA via matrix-assisted laser desorption/ionization time-of-flight mass spectrometry. *Rapid Commun. Mass Spectrom.*, **12**, 1737–1743.
20. Altman,R., Schwope,K., Sarrracino,D., Tetalaff,A., Bleczinski,C.F. and Richert,C. (1999) Selection of modified oligonucleotides with increased target affinity via MALDI-monitored nuclease survival assays. *J. Comb. Chem.*, **1**, 493–508.
21. Bruice,T.W. and Lima,W.F. (1997) Combinatorial screening and rational optimisation for hybridisation to folded hepatitis C virus RNA of oligonucleotides with biological antisense activity. *Biochemistry*, **36**, 5004–5019.
22. Ho,S.P., Britton,D.H.O., Stone,B.A., Behrens,D.L., Leffet,L.M. and Hobbs,F.W (1996) Potent antisense oligonucleotides to the human multidrug resistance-1 mRNA are rationally selected by mapping RNA-accessible sites with oligonucleotide libraries. *Nucleic Acids Res.*, **24**, 1901–1907.
23. Matveeva,O., Felden,B., Tsodikov,A., Johnston,J., Monia,B.P., Atkins,J.F., Gestelan,R.F. and Freier,S.M. (1998) Prediction of antisense oligonucleotide efficacy by *in vitro* methods. *Nat. Biotechnol.*, **16**, 1374–1375.
24. Lima,W.F., Brown-Driver,V., Fox,M., Hanecak,R. and Bruice,T.W. (1997) Combinatorial screening and rational optimization for hybridization to folded hepatitis C virus RNA of oligonucleotides with biological antisense activity. *J. Biol. Chem.*, **272**, 626–638.
25. Giles,R.V., Spiller,D.G. and Tidd,D.M. (2000) Chimeric oligodeoxynucleotide analogs: chemical synthesis, purification and molecular and cellular biology protocols. *Methods Enzymol.*, **313**, 95–135.
26. Hogrefe,R.I. Reynolds,M.A., Vaghefi,M.M., Young,K.M., Riley,T.A., Klein,R.E. and Arnold,L.J.,Jr (1993) An improved method for the synthesis and deprotection of methylphosphonate oligonucleotides. In Agrawal,S. (ed.), *Methods in Molecular Biology*. Humana Press, Totowa, NJ, Vol. 20, pp. 143.
27. Hogrefe,R.I., Vaghefi,M.M., Reynolds,M.A., Young,K.M. and Arnold,L.J.,Jr (1993) Deprotection of methylphosphonate oligonucleotides using a novel one-pot procedure. *Nucleic Acids Res.*, **21**, 2031–2038.
28. Giles,R.V., Spiller,D.G., Grzybowski,J., Clark,R.E., Nicklin,P. and Tidd,D.M. (1998) Selecting optimal oligonucleotide composition for maximal antisense effect following streptolysin O-mediated delivery into human leukaemia cells. *Nucleic Acids Res.*, **26**, 1567–1575.
29. Sambrook,J., Fritsch,E. F. and Maniatis,T. (1989) *Molecular Cloning: A Laboratory Manual*, 2nd edn. Cold Spring Harbour Laboratory Press, Cold Spring Harbour, NY.
30. Piatak,M.,Jr, Luk,K.C., Williams,B. and Lifson,J.D. (1993) Quantitative competitive polymerase chain reaction for accurate quantitation of HIV DNA and RNA species. *Biotechniques*, **14**, 70–81.
31. Zuker,M. (1989) On finding all suboptimal foldings of an RNA molecule. *Science*, **244**, 48–52.
32. Mathews,D.H., Sabina,J., Zuker,M. and Turner,D.H. (1999) Expanded sequence dependence of thermodynamic parameters improves prediction of RNA secondary structure. *J. Mol. Biol.*, **288**, 911–940.
33. Mathews,D.H., Burkard,M.E., Freier,S.M. and Wyatt,J.R. and Turner,D.H. (1999) Predicting oligonucleotide affinity to nucleic acid targets. *RNA*, **5**, 1458–1469.
34. Inoue,H., Hayase,Y., Iwai,S. and Ohtsuka,E. (1987) Sequence-dependent hydrolysis of RNA using modified oligonucleotide splints and RNase H. *FEBS Lett.*, **215**, 327–330.
35. Crooke,S.T., Lemonidis,K.M., Neilson,L., Griffey,R., Lesnik,E.A. and Monia,B.P. (1995) Kinetic characteristics of *Escherichia coli* RNase H1: cleavage of various antisense oligonucleotide–RNA duplexes. *Biochem. J.*, **312**, 599–608.
36. Denman,R.B. (1996) Facilitator oligonucleotides increase ribozyme RNA binding to full-length RNA substrates *in vitro*. *FEBS Lett.*, **382**, 116–120.
37. Wu,H., Lima,W.F. and Crooke,S.T. (1999) Properties of cloned and expressed human RNase H1. *J. Biol. Chem.*, **274**, 28270–28278.
38. Miraglia,L., Geiger,T., Bennett,C.F. and Dean,N.M. (1996) Inhibition of interleukin-1 type I receptor expression in human cell-lines by an antisense phosphorothioate oligodeoxynucleotides. *Int. J. Immunopharmacol.*, **18**, 227–240.
39. Monia,B.P., Johnston,J.F., Geiger,T., Muller,M. and Fabbro,D. (1996) Antitumor activity of a phosphorothioate antisense oligodeoxynucleotide targeted against C-raf kinase. *Nature Med.*, **2**, 668–675.
40. Peyman,A., Helsberg,M., Kretzschmar,G., Mag,M., Grabley,S. and Uhlmann,E. (1995) Inhibition of viral growth by antisense oligonucleotides directed against the IE110 and the UL30 mRNA of herpes simplex virus type-1. *Biol. Chem. Hoppe Seyler*, **376**, 195–198.
41. Herschlag,D. (1991) Implications of ribozyme kinetics for targeting the cleavage of specific RNA molecules *in vivo*: more isn't always better. *Proc. Natl Acad. Sci. USA*, **88**, 6921–6925.
42. Wagner,R.W., Matteucci,M.D., Grant,D., Huang,T. and Froehler,B.C. (1996) Potent and selective inhibition of gene expression by an antisense heptanucleotide. *Nat. Biotechnol.*, **14**, 840–844.
43. Zheng,Z.M. and Specter,S. (1996) Dynamic production of tumour necrosis factor-α (TNF-α) messenger RNA, intracellular and extracellular TNF-α by murine macrophages and possible association with protein tyrosine phosphorylation of STAT1α and ERK2 as an early signal. *Immunology*, **87**, 544–550.
44. Hartmann,G. and Krieg,A.M. (1999) CpG DNA and LPS induce distinct patterns of activation in human monocytes. *Gene Ther.*, **6**, 893–903.
45. Krieg,A.M., Matson,S., Cheng,K., Fisher,E., Koretzky,G.A. and Koland,J.G. (1997) Identification of an oligodeoxynucleotide sequence motif that specifically inhibits phosphorylation by protein tyrosine kinases. *Antisense Nucleic Acid Drug Dev.*, **7**, 115–123.
46. Hu,R.H. and Chu,S.H. (2000) Suppression of tumor necrosis factor secretion from white blood cells by synthetic antisense phosphorothioate oligodeoxynucleotides. *Int. J. Pharmacol.*, **22**, 445–452.
47. Hartmann,G., Krug,A., Waller Fontaine,K. and Endres,S. (1996) Oligodeoxynucleotides enhance lipopolysaccharide-stimulated synthesis of tumor necrosis factor: dependence on phosphorothioate modification and reversal by heparin. *Mol. Med.*, **2**, 429–438.
48. Taylor,M.F., Paulauskis,J.D., Weller,D.D. and Korbzik,L. (1997) Comparison of efficacy of antisense oligomers directed toward TNF-α in helper T and macrophage cell lines. *Cytokine*, **9**, 672–681.
49. Tu,G., Cao,Q., Zhou,F. and Israel,Y. (1998) Tetranucleotide GGGA motif in primary RNA transcripts. *J. Biol. Chem.*, **273**, 25125–25131.
50. Matveeva,O.V., Tsodikov,A.D., Giddings,M., Freier,S.M., Wyatt,J.R., Spiridonov,A.N. Shabalina,S.A., Gesteland,R.F. and Atkins,J.F. (2000) Identification of sequence motifs in oligonucleotides whose presence is correlated with antisense activity. *Nucleic Acids Res.*, **28**, 2862–2865.